ACS APPLIED MATERIALS & INTERFACES

Research Article

www.acsami.org

# Influence of the Terminal Electron Donor in D−D−π−A Organic Dye-Sensitized Solar Cells: Dithieno[3,2-b:2′,3′-d]pyrrole versus Bis(amine)

Panpan Dai,[†] Lin Yang,[§] Mao Liang,*[,†,‡] Huanhuan Dong,[†] Peng Wang,*[,§] Chunyao Zhang,[†] Zhe Sun,[†] and Song Xue[†]

[†]Tianjin Key Laboratory of Organic Solar Cells and Photochemical Conversion, Department of Applied Chemistry, Tianjin University of Technology, Tianjin 300384, People's Republic of China

[‡]Key Laboratory of Advanced Energy Materials Chemistry (Ministry of Education), Collaborative Innovation Center of Chemical Science and Engineering, College of Chemistry, Nankai University, Tianjin 300071, People's Republic of China

[§]State Key Laboratory of Polymer Physics and Chemistry Changchun Institute of Applied Chemistry, Chinese Academy of Sciences No. 5625, Ren Min Street, Changchun 130022, People's Republic of China

Supporting Information

**ABSTRACT:** With respect to the electron-withdrawing acceptors of D−A−π−A organic dyes, reports on the second electron-donating donors for D−D−π−A organic dyes are very limited. Both of the dyes have attracted significant attention in the field of dye-sensitized solar cells (DSCs). In this work, four new D−D−π−A organic dyes with dithieno[3,2-b:2′,3′-d]pyrrole (DTP) or bis(amine) donor have been designed and synthesized for a investigation of the influence of the terminal electron donor in D−D−π−A organic dye-sensitized solar cells. It is found that DTP is a promising building block as the terminal electron donor when introduced in the dithiophenepyrrole direction, but not just a good bridge, which exhibits several characteristics: (i) efficiently increasing the maximum molar absorption coefficient and extending the absorption bands; (ii) showing stronger charge transfer interaction as compared with the pyrrole direction; (iii) beneficial to photocurrent generation of DSCs employing cobalt electrolytes. DSCs based on M45 with the Co-phen electrolyte exhibit good light-to-electric energy conversion efficiencies as high as 9.02%, with a short circuit current density ($J_{SC}$) of 15.3 mA cm$^{-2}$, open circuit voltage ($V_{OC}$) of 867 mV and fill factor (FF) of 0.68 under AM 1.5 illumination (100 mW cm$^{-2}$). The results demonstrate that N,S-heterocycles such as DTP unit could be promising candidates for application in highly efficient DSCs employing cobalt electrolyte.

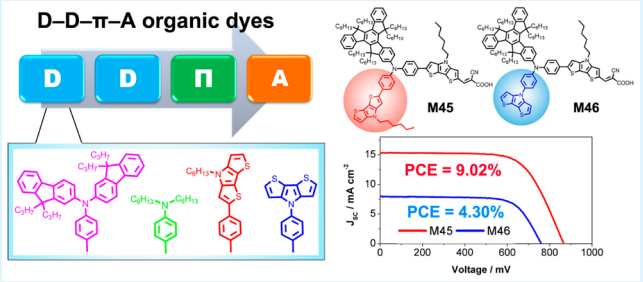


**KEYWORDS:** *dye-sensitized solar cells, D−D−π−A organic dyes, electron donor, dithieno[3,2-b:2′,3′-d]pyrrole, photovoltaic performance*

## INTRODUCTION

Dye-sensitized solar cells (DSCs), a hybrid organic−inorganic system, are considered one of the most promising photovoltaic devices due to their low manufacturin cost, excellent photovoltaic performance and high versatility.[1−28] A recent breakthrough in DSC research has been the successful application of transition-metal complexes such as cobalt(II/III) polypyridyl redox couples as alternatives, replacing formerly used corrosive iodine/iodide electrolytes while maintaining impressive energy conversion efficiencies.[29−33] Using a zinc porphyrin dye SM315 with the cobalt(II/III) redox shuttle resulted in dye-sensitized solar cells that exhibit a high open-circuit voltage of 0.91 V, short-circuit current density of 18.1 mA cm$^{-2}$, fill factor of 0.78 and a power conversion efficiency (PCE) of 13%.[33] Meanwhile, much effort has also been devoted to the design and synthesis of metal free organic dyes toward cobalt electrolytes, which currently reach more than 12% PCE.[34−37]

Generally, metal-free organic sensitizers are constituted by donor (D), π-bridge (π) and acceptor (A) moieties, so-called D−π−A character, which induces the intramolecular charge transfer (ICT) from subunit A to D through the π-bridge when a dye absorbs light.[3] This recognition has translated into a great deal of effort in designing different kinds of organic dyes based on this basic mode. Apart from the D−π−A configuration, other typical modes such as D−D−π−A and D−A−π−A have also been developed and attracted more attention (Figure 1). Ning et al. found that the introduction of starburst triarylamine

Received: July 17, 2015
Accepted: September 22, 2015
Published: September 22, 2015




DOI: 10.1021/acsami.5b06481
ACS Appl. Mater. Interfaces 2015, 7, 22436−22447

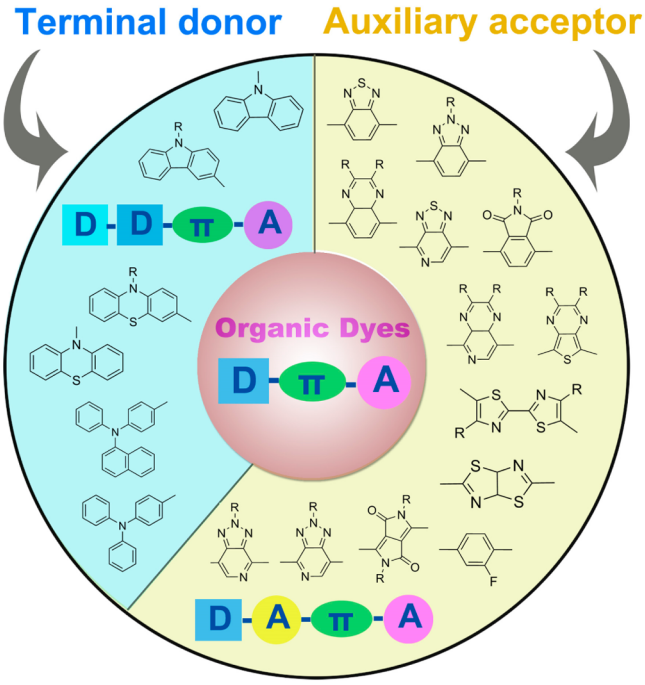


**Figure 1.** Configuration of D−$\pi$−A, D−D−$\pi$−A and D−A−$\pi$−A organic dyes as well as the typical building blocks for the terminal donor and the auxiliary acceptor.

group to form the D−D−$\pi$−A configuration brought about superior performance over the simple D−$\pi$−A configuration, in terms of bathochromically extended absorption spectra, enhanced molar extinction coefficients and better thermostability.[38] On the other hand, the D−A−$\pi$−A configuration displays several advantages such as tuning of the molecular energy levels, red-shift of the charge-transfer absorption band, and distinct improvement of photovoltaic performance and stability.[39] The D−A−$\pi$−A strategy to organic dyes has been developed and well-studied in Lin's, Zhu's, Wang's, Hua's and other groups.[39] To date, many electron-withdrawing acceptors such as benzothiadiazole,[40−42] benzotriazole,[43] 2H-[1,2,3]-triazolo[4,5-*c*]pyridine,[44] [1,2,5]thiadiazolo[3,4-*c*]pyridine,[45] quinoxaline,[46−48] phthalimide,[49] diketopyrrolopyrrole,[50] pyrido[3,4-*b*]pyrazine,[51] thienopyrazine,[52] thiazolo[5,4-*d*]-thiazole,[53,54] bithiazole,[55] fluoro-substituted phenyl[56] and disubstituted cyclopenta[1,2-b:5,4-b′]dithiophene[57] have been introduced as the auxiliary acceptor in D−A−$\pi$−A organic dyes, resulting in novel organic dyes with promising performance. By contrast, reports on exploration of new electron-donating donors (carbazole,[25,58−62] phenothiazine,[63,64] naphthylphenylamino,[65] triarylamine[66−68]) for D−D−$\pi$−A organic dyes are very limited. There is much room left for further development of D−D−$\pi$−A organic dyes by incorporating of different terminal electron donor.

With this in mind, we incorporate the *N*,*N*-difluorenebenzenamine (DFBA), *N*,*N*-dihexylbenzenamine (DHBA), benzenehexyldithieno[3,2-b:2′,3′-d]pyrrole (DTP) (BZ-HDTP) and benzene-substituted DTP (BZDTP) as the terminal electron donors to construct four novel D−D−$\pi$−A organic dyes (M43−46, see Figure 2). In particular, the DTP unit was introduced as electron donor in two perpendicular directions, i.e., the dithiophenepyrrole direction (M45) or the pyrrole direction (M46). As shown in Figure 1, carbazole and phenothiazine can also be incorporated in two different directions at the end of the organic dyes. Nevertheless, to the best of knowledge, reports on influence of the donor direction (carbazole/phenothiazine) on the performance of the D−D−$\pi$−A dyes are lacking. It is expected that these electron donors could have a major impact on the photophysical, electrochemical properties and photovoltaic parameters of dyes, which will be further scrutinized via a joint photophysical and electrical analysis.

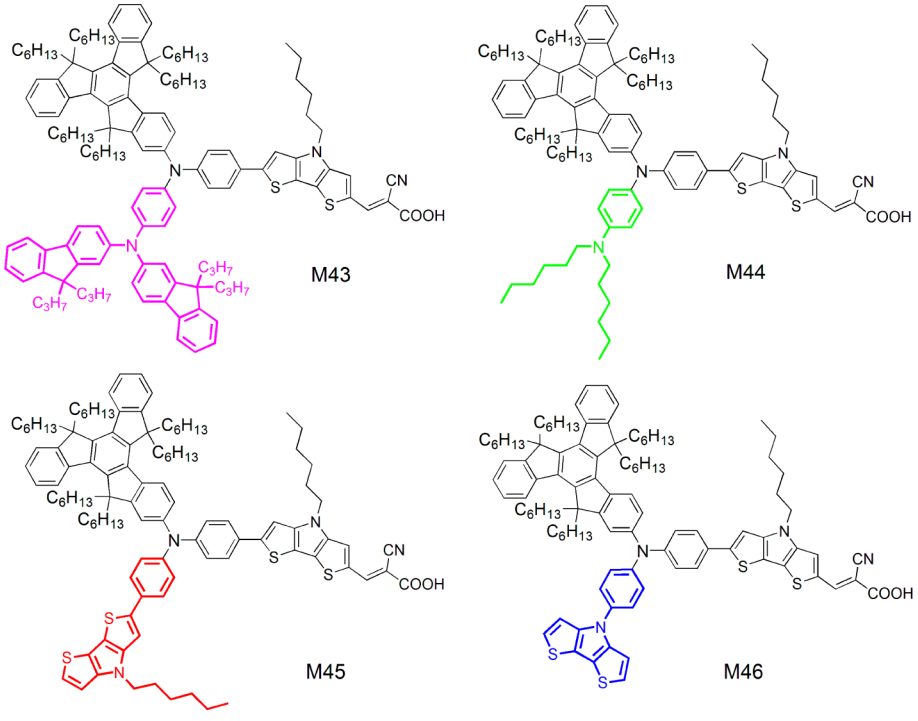


**Figure 2.** Chemical structures of the M43−46.


DOI: 10.1021/acsami.5b06481
*ACS Appl. Mater. Interfaces* 2015, 7, 22436−22447

**Scheme 1. Schematic Diagram for the Synthesis of the Studied Dyes**

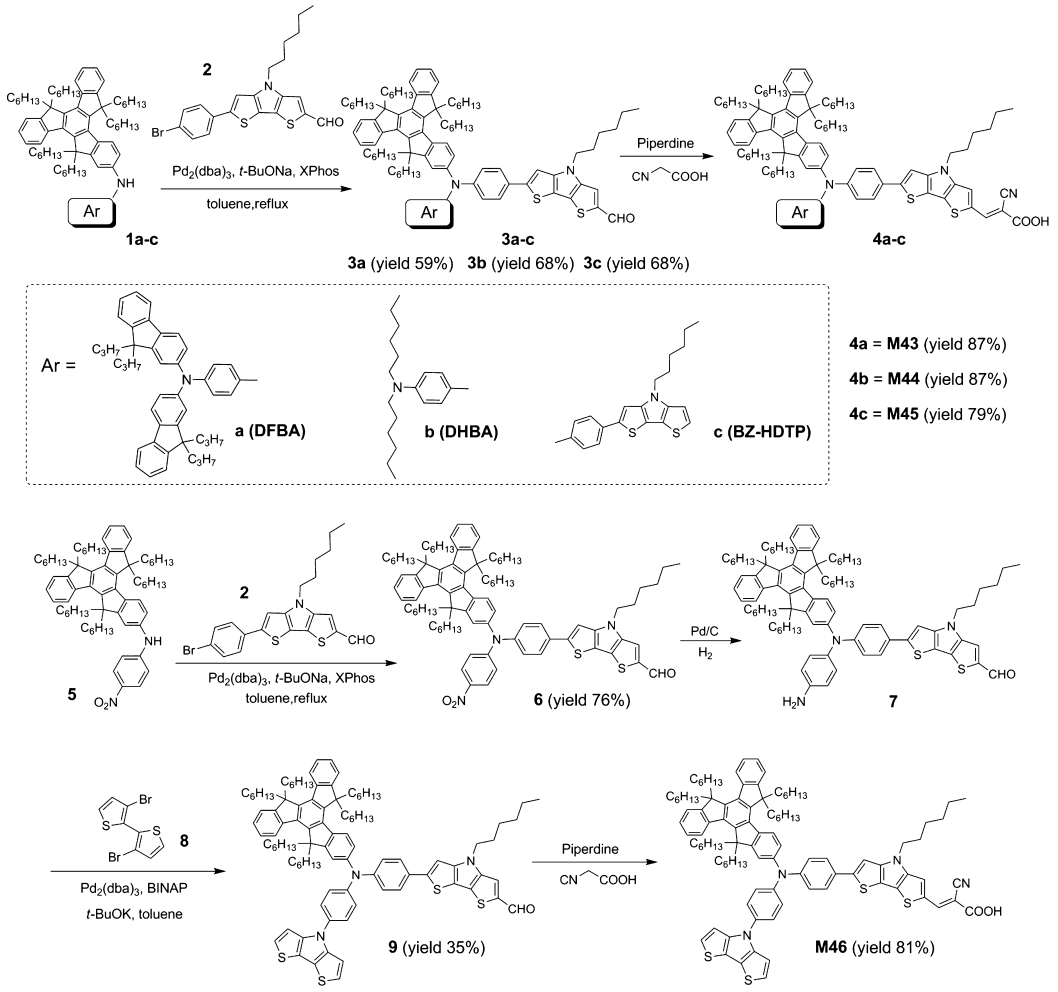


## EXPERIMENTAL SECTION

**Materials and Instruments.** The synthetic routes for the five dyes are shown in Scheme 1. $Pd_2(dba)_3$, Xphos, BINAP, *t*-BuONa and cyanocertic acid were purchased from Energy Chemical (China). 4-*tert*-Butylpyridine (TBP) and lithium bis(trifluoromethanesulfonyl)-imide (LiTFSI) were purchased from Aldrich. *N*,*N*-Dimethylformamide was dried over and distilled from $CaH_2$ under an atmosphere of nitrogen. Phosphorus oxychloride was freshly distilled before use. Dichloromethane was distilled from calcium hydride under nitrogen atmosphere. All other solvents and chemicals used in this work were analytical grade and used without further purification.

$^1$H NMR and $^{13}$C NMR spectra were recorded on a Bruker AM-300 or AM-400 spectrometer. The reported chemical shifts were against TMS. High resolution mass spectra were obtained with a Micromass GCT-TOF mass spectrometer. The melting point was taken on a RY-1 thermometer, and temperatures were uncorrected.

**Synthesis of Dyes.** *General Synthesis Procedure of Dyes.* To a stirred solution of carbaldehyde (0.2 mmol) and cyanoacetic acid (0.3 mmol) in acetonitrile (8 mL) were added chloroform (4 mL) and piperidine (0.6 mmol). The reaction mixture was refluxed for 8 h. Additional cyanoacetic acid (0.2 mmol) and piperdine (0.4 mmol) were added. The mixture was refluxed for 8 h and then acidified with 1 M hydrochloric acid aqueous solution (30 mL). The crude product was extracted into $CH_2Cl_2$, washed with water, and dried over anhydrous $MgSO_4$. The solvent was evaporated, and the remaining crude product was purified by column chromatography ($CH_2Cl_2$:methanol = 20:1 as eluent) to give the product.

**M43**. Red power (yield: 87%). MP: 125−129 °C. $^1$H NMR (400 MHz, $CDCl_3$+MeOD-$d_4$): $\delta$ 8.36 (d, $J$ = 7.38 Hz, 1H), 8.35−8.26 (m, 3H), 7.72 (s, 1H), 7.63−7.55 (m, 6H), 7.46−7.44 (m, 2H), 7.39−7.35 (m, 4H), 7.27 (s, 1H), 7.31 (s, 3H), 7.26 (s, 1H), 7.25−7.20 (m, 5H), 7.18 (d, $J$ = 11.35 Hz, 2H), 7.13−7. 09 (m, 7H), 4.25 (t, $J$ = 6.24 Hz, 2H), 3.00−2.84 (m, 6H), 2.10−2.00 (m, 4H), 2.02−1.96 (m, 12H), 1.29 (t, $J$ = 4.24 Hz, 6H), 096−0.86 (m, 39H), 0.68−0.50 (m, 50H). $^{13}$C NMR (100 MHz, $CDCl_3$): 155.17, 153.65, 153.54, 149.29, 146.15, 144.67, 144.23, 144.13, 141.03, 140.43, 140.32, 138.83, 138.34, 138.26, 138.10, 137.95, 126.54, 126.28, 125.95, 125.43, 125.30, 124.65, 123.80, 122.49, 122.17, 121.85, 121.55, 120.49, 118.89, 118.61, 117.43, 113.66, 109.59, 108.89, 55.65, 55.56, 55.51, 47.54, 43.34, 36.98, 36.80, 31.61, 31.51, 31.46, 31.40, 30.17, 29.71, 29.54, 29.49, 29.40, 29.14, 29.06, 27.04, 26.66, 24.07, 23.92, 23.77, 22.59, 22.51, 22.38. HRMS (EIS) calcd for $C_{131}H_{157}N_4O_2S_2$ ($M + H^+$): 1882.1748. Found: 1882.1763.

**M44**. Red power (yield: 87%). MP: 114−118 °C. $^1$H NMR (400 MHz, $CDCl_3$+MeOD-$d_4$): $\delta$ 8.37−8.21 (m, 4H), 7.78 (s, 1H), 7.58 (d, $J$ = 8.37 Hz, 1H), 7.48−7.44 (m, 3H), 7.39−7.34 (m, 5H), 7.24−7.04 (m, 7H), 6.67 (s, 1H), 4.23 (t, $J$ = 8.23 Hz, 2H), 3.29 (s, 2H), 3.03 (t, $J$ = 7.59 Hz, 2H), 2.97−2.87 (m, 6H), 2.08−1.91 (m, 8H), 1.36−1.27 (m, 21H), 1.02−0.87 (m, 46H), 0.70−0.51 (m, 30H). $^{13}$C NMR (100 MHz, $CDCl_3$): 155.03, 153.54, 145.86, 145.17, 144.88, 144.67, 144.50, 144.31, 144.08, 140.44, 140.34, 140.23, 138.43, 138.30, 138.24, 137.90, 127.66, 126.64, 126.26, 125.92, 125.36, 124.63, 124.57, 122.87, 122.15, 121.13, 120.34, 113.53, 113.11, 104.82, 55.61, 55.53, 55.50, 53.40, 36.98, 36.82, 31.92, 31.77, 31.74, 31.56, 31.49, 31.45, 31.41, 31.37, 30.80, 30.31, 30.15, 29.69, 29.65, 29.60, 29.51, 29.47, 29.39, 29.35, 29.26, 29.10, 27.22, 27.14, 26.93, 26.88, 26.63, 25.95, 25.89, 24.76, 24.11, 24.01, 23.90, 23.77, 22.70, 22.48, 22.36, 22.28, 22.25, 18.65, 13.96. HRMS (EIS) calcd for $C_{105}H_{141}N_4O_2S_2$ ($M + H^+$): 1555.0429. Found: 1555.0616.



DOI: 10.1021/acsami.5b06481
*ACS Appl. Mater. Interfaces* 2015, 7, 22436−22447

**M45**. Red power (yield: 79%). MP: 119−121 °C. $^1$H NMR (400 MHz, $CDCl_3$+MeOD-$d_4$): $\delta$ 8.37 (d, $J$ = 7.79 Hz, 1H), 8.29 (t, $J$ = 8.34 Hz, 3H), 7.77 (s, 1H), 7.61−7.58 (m, 4H), 7.48−7.44 (m, 2H), 7.40−7.37 (m, 4H), 7.32 (d, $J$ = 2.08 Hz, 1H), 7.25 (d, $J$ = 8,83 Hz, 4H), 7.22 (s, 1H), 7.18 (s, 2H), 7.15 (d, $J$ = 5.19 Hz, 1H), 7.01 (d, $J$ = 5.71 Hz, 1H), 4.26−4.21 (m, 4H), 3.02−2.89 (m, 6H), 2.12−2.03 (m, 4H), 1.97−1.87 (m, 6H), 1.33−1.30 (m, 12H), 0.97−0.86 (m, 42H), 0.72−0.68 (m, 12H), 0.62 (t, $J$ = 7.59 Hz, 9H), 0.57−0.50 (m, 9H). $^{13}$C NMR (100 MHz, $CDCl_3$): 155.45, 153.63, 153.49, 146.24, 145.27, 145.14, 144.65, 144.55, 144.33, 141.25, 140.34, 140.21, 138.45, 126.54, 126.37, 126.20, 125.99, 125.58, 124.59, 123.01, 115.03, 113.84, 110.89, 106.35, 55.71, 55.59, 55.52, 47.42, 36.95, 36.79, 31.94, 31.58, 31.50, 30.38, 30.20, 29.71, 29.67, 29.48, 29.38, 29.27, 26.70, 26.65, 24.06, 23.91, 23.77, 22.52, 23.38, 22.89, 22.26, 14.13, 14.01, 13.90. HRMS (EIS) calcd for $C_{107}H_{131}N_4O_2S_4$ (M + H$^+$): 1631.9155. Found: 1631.9180.

**M46**. Red power (yield: 81%). MP: 118−122 °C. $^1$H NMR (400 MHz, $CDCl_3$+MeOD-$d_4$): $\delta$ 8.36 (d, $J$ = 6.57 Hz, 1H), 8.27 (d, $J$ = 8.57 Hz, 1H), 8.24−8.16 (m, 2H), 7.65 (s, 1H), 7.54 (d, $J$ = 8.56 Hz, 1H), 7.47 (d, $J$ = 8.76 Hz, 2H), 7.44−7.42 (m, 3H), 7.36−7.32 (m, 6H), 7.26−7.00 (m, 8H), 6.62 (d, $J$ = 8.26 Hz, 1H), 4.25 (t, $J$ = 6.88 Hz, 2H), 2.96−2.89 (m, 6H), 2.07−1.99 (m, 4H), 1.93−1.85 (m, 4H), 1.33−1.26 (m, 6H), 0.95−0.84 (m, 39H), 0.66−0.49 (m, 30H). $^{13}$C NMR (100 MHz, $CDCl_3$): 155.45, 153.63, 153.49, 146.24, 145.27, 145.14, 144.65, 144.55, 144.33, 141.25, 140.34, 140.21, 138.45, 138.31, 137.89, 130.58, 128.82, 126.55, 126.37, 126.20, 125.99, 125.58, 124.59, 123.01, 122.21, 115.03, 113.84, 110.89, 106.35, 55.71, 55.59, 55.52, 47.42, 36.95, 36.79, 31.94, 31.58, 31.50, 31.45, 30.38, 30.20, 29.71, 29.67, 29.48, 29.38, 29.27, 26.70, 26.65, 24.06, 23.91, 23.77, 22.52, 22.38, 22.28, 22.26, 14.13, 14.01, 13.90. HRMS (EIS) calcd for $C_{101}H_{119}N_4O_2S_4$ (M + H$^+$): 1547.8215. Found: 1547.8218.

*General Synthesis Procedure of Compounds **3a−c** and **6**.* To a 100 mL two-neck round-bottomed flask were added 20 mL anhydrous toluene, compounds **1a−c** (400.0 mg, 0.36 mmol), compound **2** (230.1 mg, 0.54 mmol), anhydrous sodium tert-butoxide (100.6 mg, 1.08 mmol), tris(dibenzylideneacetone) dipalladium (16.4 mg, 18.00 $\mu$mol) and XPhos (17.2 mg, 36.01 $\mu$mol). The mixture was refluxed for 24 h in the dark under argon. After the solution cooled to room temperature, $H_2O$ and ethyl acetate were added. The organic layer was separated and dried in $Na_2SO_4$. The solvent was evaporated and the remaining crude product was purified by column chromatography (PE:EA = 20:1 as eluent).

**3a**. Brown solid (yield: 59%). MP: 72−74 °C. $^1$H NMR (400 MHz, $CDCl_3$): $\delta$ 9.89 (s, 1H), 8.38 (d, $J$ = 7.15 Hz, 1H), 8.33 (d, $J$ = 7.94 Hz, 1H), 8.29 (d, $J$ = 8.61 Hz, 1H), 7.65 (q, $J$ = 7.33 Hz, 4H), 7.62 (d, $J$ = 4.95 Hz, 2H), 7.59 (s, 1H), 7.48 (t, $J$ = 2.12 Hz, 2H), 7.45−7.39 (m, 4H), 7.35 (t, $J$ = 7.40 Hz, 6H), 7.30 (s, 1H), 7.27 (s, 3H), 7.24 (d, $J$ = 1.77 Hz, 1H), 7.21 (s, 1H), 7.18 (d, $J$ = 5.50 Hz, 4H), 7.16 (s, $J$ = 1.27 Hz, 2H), 7.14 (d, $J$ = 1.43 Hz, 1H), 4.26 (t, $J$ = 7.03 Hz, 2H), 3.01−2.90 (m, 6H), 2.13−2.00 (m, 4H), 1.99−1.86 (m, 12H), 1.36−1.31(m, 6H), 1.01−0.91 (m, 39H), 0.83−0.73 (m, 18H), 0.73−0.60 (m, 24H), 0.54 (q, $J$ = 15.10 Hz, 8H). $^{13}$C NMR (100 MHz, $CDCl_3$): $\delta$ 182.72, 153.67, 153.48, 152.11, 150.49, 149.77, 144.64, 144.42, 144.24, 143.83, 140.96, 140.39, 140.27, 139.75, 138.42, 138.29, 136.00, 126.83, 124.68, 124.58, 123.80, 122.79, 122.57, 122.34, 122.16, 120.36, 119.05, 118.40, 105.36, 55.66, 55.59, 55.53, 55.25, 47.50, 42.69, 36.97, 36.85, 31.56, 31.51, 31.46, 31.41, 30.27, 29.52, 29.49, 29.41, 26.70, 24.04, 23.92, 23.77, 22.51, 22.34, 22.27, 17.35, 14.60, 14.01, 13.98, 13.96, 13.91. HRMS (EIS) calcd for $C_{128}H_{156}N_3OS_2$ (M + H$^+$): 1816.1722. Found: 1816.1733.

**3b**. Brown solid (yield: 68%). MP: 71−75 °C. $^1$H NMR (400 MHz, $CDCl_3$): $\delta$ 9.88 (s, 1H), 8.38 (d, $J$ = 7.24 Hz, 1H), 8.32 (d, $J$ = 6.43 Hz, 1H), 8.29 (d, $J$ = 8.37 Hz, 1H), 7.65 (q, $J$ = 4.84 Hz, 1H), 7.53 (d, $J$ = 8.68 Hz, 2H), 7.46 (q, $J$ = 7.20 Hz, 3H), 7.41−7.35 (m, 4H), 7.19−7.10 (m, 6H), 6.66 (d, $J$ = 8.42 Hz, 2H), 4.25 (t, $J$ = 7.00 Hz, 2H), 3.30 (s, 4H), 3.00−2.88 (m, 6H), 2.13−2.00 (m, 4H), 1.96−1.90 (m, 4H), 1.37−1.33 (m, 21H), 1.03−0.88 (m, 46H), 0.71−0.52 (m, 30H). $^{13}$C NMR (100 MHz, $CDCl_3$): 182.60, 153.68, 153.56, 149.92, 149.73, 148.22, 147.76, 147.52, 145.82, 145.46, 145.27, 144.64, 144.05, 143.86, 143.74, 140.46, 140.38, 138.32, 138.25, 135.04, 127.88, 126.37, 126.28, 125.94, 125.37, 124.64, 124.59, 123.87, 122.16, 121.66, 121.11, 119.03, 117.16, 113.32, 112.55, 104.93, 55.62, 55.56, 55.51, 53.81, 51.33, 47.47, 37.00, 36.85, 31.79, 31.58, 31.52, 31.48, 31.41, 30.26, 29.53, 29.49, 29.42, 26.92, 26.70, 24.03, 23.92, 23.79, 22.74, 22.51, 22.38, 22.30, 22.27, 14.13, 14.07, 13.90. HRMS (EIS) calcd for $C_{104}H_{140}N_3OS_2$ (M + H$^+$): 1488.0471. Found: 1488.0568.

**3c**. Brown solid (yield: 68%). MP: 72−73 °C. $^1$H NMR (400 MHz, $CDCl_3$): $\delta$ 9.89 (s, 1H), 8.38 (d, $J$ = 7.66 Hz, 1H), 8.31 (d, $J$ = 8.28 Hz, 2H), 7.69 (d, $J$ = 7.09 Hz, 1H), 7.66 (s, 1H), 7.61 (q, $J$ = 8.78 Hz, 4H), 7.49−7.43 (m, 3H), 7.42−7.36 (m, 4H), 7.33 (d, $J$ = 2.19 Hz, 1H), 7.27 (s, 1H), 7.25 (d, $J$ = 2.31 Hz, 2H), 7.23 (s, 1H), 7.20 (s, 1H), 7.16 (d, $J$ = 4.99 Hz, 1H), 7.03 (d, $J$ = 5.35 Hz, 1H), 4.28−4.22 (m, 4H), 3.01−2.88 (m, 6H), 2.14−2.03 (m, 4H), 1.98−1.89 (m, 6H), 1.37−1.33 (m, 12H), 0.99−0.88 (m, 42H), 0.72−0.67 (m, 11H), 0.63 (t, $J$ = 6.32 Hz, 10H), 0.57−0.52 (m, 9H). $^{13}$C NMR (100 MHz, $CDCl_3$): 182.70, 155.43, 153.65, 149.72, 147.73, 147.50, 146.33, 145.28, 144.67, 144.33, 143.89, 141.29, 140.35, 140.29, 149.23, 139.85, 138.46, 138.32, 137.91, 136.37, 130.59, 129.08, 128.76, 128.21, 126.59, 126.36, 125.98, 125.80, 125.58, 124.68, 124.58, 124.51, 123.77, 123.49, 123.02, 122.81, 122.22, 118.561, 15.04, 113.86, 113.75, 110.89, 106.69, 105.58, 58.46, 55.72, 55.60, 55.54, 47.50, 47.44, 36.96, 36.82, 31.57, 31.50, 31.43, 31.39,30.36, 30.61, 129.49, 29.46, 29.38, 26.69, 24.06, 23.91, 23.76, 22.51, 22.49, 22.39, 22.28, 22.25, 18.43, 13.98, 13.88. HRMS (EIS) calcd for $C_{104}H_{130}N_3OS_4$ (M + H$^+$): 1564.9097. Found: 1564.9098.

**6**. Orange solid (yield: 76%). MP: 82−83 °C. $^1$H NMR (400 MHz, $CDCl_3$): $\delta$ 9.90 (s, 1H), 8.39 (t, $J$ = 7.09 Hz, 2H), 8.31 (d, $J$ = 7.76 Hz, 1H), 8.14 (d, $J$ = 9.21 Hz, 2H), 7.71 (s, 1H), 7.69 (s, 1H), 7.67 (s, 1H), 7.51−7.46 (m, 2H), 7.43−7.38 (m, 4H), 7.33 (q, $J$ = 13.71 Hz, 2H), 7.31 (s, 1H), 7.26 (s, 1H), 7.21 (q, $J$ = 8.36 Hz, 1H), 7.17 (d, $J$ = 9.29 Hz, 2H), 4.28 (t, $J$ = 6.79 Hz, 2H), 3.01−2.87 (m, 6H), 2.1−2.08 (m, 4H), 2.00−1.91 (m, 4H), 1.42−1.33 (m, 6H), 1.06−0.80 (m, 39H), 0.68 (q, $J$ = 12.87 Hz, 12H), 0.63 (t, $J$ = 6. 97, Hz, 8H), 0.58−0.50 (m, 10H). $^{13}$C NMR (100 MHz, $CDCl_3$): 161.96, 153.64, 153.39, 153.31, 145.25, 145.14, 144.97, 144.74, 142.54, 140.54, 140.48, 140.20, 140.03, 126.31, 126.06, 125.93, 125.47, 125.13, 124.73, 124.55, 124.19, 123.42, 122.29, 122.19, 121.64, 118.84, 110.89, 107.07, 55.85, 55.71, 55.60, 47.45, 36.94, 36.91, 36.78, 31.51, 31.47, 31.40, 30.33, 29.42, 29.31, 28.84, 26.67, 24.07, 23.91, 23.76, 22.47, 22.28, 13.91, 13.87, 13.82. HRMS (EIS) calcd for $C_{90}H_{114}N_3O_3S_2$ (M + H$^+$): 1348.8302. Found: 1348.8356.

*Synthesis of Compound **9**.* Compound **6** (500 mg, 0.376 mmol) was dissolved in 100 mL of absolute THF, then 10% Pd/C (40.01 mg, 37.6 $\mu$mol) catalyst was added. The reaction mixture was purged with hydrogen and stirred at room temperature for 3 days. At the end of the reaction, the mixture was filtered and the filtrate was concentrated under reduced pressure. Then the precipitate were filtered and dried under vacuum. Compound **7** was obtained as a brown oil (488.5 mg, yield: 96.7%) without purification.

To a 100 mL two-neck round-bottomed flask were added 20 mL of anhydrous toluene, compound **7** (400 mg, 0.308 mmol), compound **8** (99.73 mg, 0.308 mmol), anhydrous sodium tert-butoxide (88.74 mg, 0.924 mmol), tris(dibenzylideneacetone)dipalladium (9.8 mg, 10.78 $\mu$mol) and BINAP (19.2 mg, 30.8 $\mu$mol). The reaction mixture was stirred and refluxed at Ar atmosphere overnight. The solvent was evaporated, and the remaining crude product was purified by column chromatography (PE:EA = 20:1 as eluent) to give the product. Orange solid (145 mg, yield: 35%). MP: 79−81 °C. $^1$H NMR (400 MHz, $CDCl_3$): $\delta$ 9.88 (s, 1H), 8.39 (d, $J$ = 7.19 Hz, 1H), 8.31 (d, $J$ = 6.39 Hz, 1H), 8.24 (d, $J$ = 9.35 Hz, 1H), 7.65 (s, 1H), 7.54 (d, $J$ = 8.63 Hz, 2H), 7.49−7.46 (m, 2H), 7.41−7.37 (m, 7H), 7.23 (s, 1H), 7.20 (t, $J$ = 5.40 Hz, 3H), 7.16 (d, $J$ = 1.80 Hz, 2H), 7.14 (s, 1H), 7.11 (d, $J$ = 5.40 Hz, 1H), 6.95 (d, $J$ = 8.99 Hz, 2H), 4.28 (t, $J$ = 6.83 Hz, 2H), 3.00−2.91 (m, 6H), 2.10−2.01 (m, 4H), 2.00−1.91 (m, 4H), 1.44−1.32 (m, 6H), 1.01−0.88 (m, 39H), 0.68 (t, $J$ = 7.19 Hz, 12H), 0.62 (t, $J$ = 7.19 Hz, 10H), 0.55−0.52 (m, 8H). $^{13}$C NMR (100 MHz, $CDCl_3$): 177.67, 153.64, 151.51, 144.62, 144.09, 143.77, 140.33, 138.32, 135.82, 134.36, 130.89, 128.25, 127.75, 126.3, 125.92, 125.50, 124.63, 124.56, 123.97, 122.15, 119.04, 115.88, 103.91, 98.44, 55.54, 55.50, 47.47, 36.96, 36.80, 34.22, 33.25, 32.32, 31.91, 31.62, 31.53, 31.50, 31.43, 31.37,


DOI: 10.1021/acsami.5b06481
ACS Appl. Mater. Interfaces 2015, 7, 22436−22447

**Table 1. Optical Properties and Electrochemical Properties of the Dyes**

| dye | $\lambda_{max}$ (nm)[a] | $\varepsilon$ ($10^3$ $M^{-1}cm^{-1}$) | $E_{0-0}$ (eV)[b] | HOMO (V) vs NHE[c] | HOMO (V)[d] | LUMO (V) vs NHE[e] |
|---|---|---|---|---|---|---|
| M43 | 529 | 60300 | 2.10 | 0.81 | −4.76 | −1.29 |
| M44 | 535 | 58400 | 2.10 | 0.64 | −4.71 | −1.46 |
| M45 | 521 | 79600 | 2.16 | 0.92 | −4.87 | −1.24 |
| M46 | 510 | 69300 | 2.17 | 1.03 | −5.14 | −1.14 |

[a]The absorption spectra in DCM. [b]$E_{0-0}$ values were estimated from the intersections of normalized absorption and emission spectra ($\lambda_{int}$): $E_{0-0}$ = 1240/$\lambda_{int}$. Normalized absorption and emission spectra of the dyes in dichloromethane can be found in Figure S1 in the Supporting Information. [c]HOMO was recorded by cyclic voltammograms of the dye-loaded $TiO_2$ film. [d]Theoretical HOMO data calculated at the B3LYP/6-31G level of the dyes in a vacuum. [e]LUMO was calculated from HOMO − $E_{0-0}$.

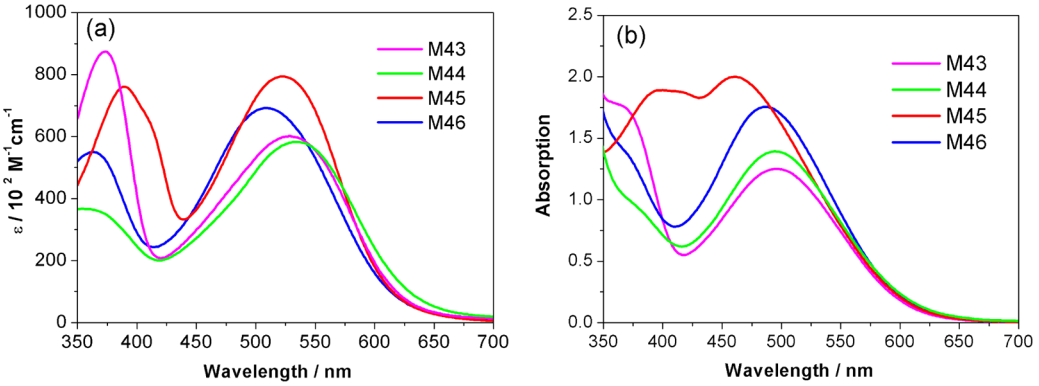


**Figure 3.** Absorption spectra of the dyes in dichloromethane (a) and the dyes sensitized film (b).

30.32, 30.23, 29.68, 29.65, 29.45, 27.77, 26.67, 24.00, 23.89, 23.75, 23.38, 22.67, 22.46, 22.32, 22.25, 22.23, 22.16, 13.95. HRMS (EIS) calcd for $C_{98}H_{118}N_3OS_4$ (M + $H^+$): 1480.8158. Found: 1480.8130.

**Optical and Electrochemical Measurements.** The absorption spectra of dyes and sensitized films were measured by SHIMADZU UV-2600 spectrophotometer. Fluorescence measurements were carried out with a HITACHI F-4500 fluorescence spectrophotometer.

Cyclic voltammetry (CV) measurements for sensitized films were performed on a Zennium electrochemical workstation (ZAHNER, Germany), with sensitized electrodes as the working electrode, Pt-wires as the counter electrode and an Ag/AgCl electrode as the reference electrode at a scan rate of 10 mV $s^{-1}$. Tetrabutylammonium perchlorate (TBAP, 0.1 M) and MeCN were used as the supporting electrolyte and solvent, respectively. The results were calibrated using ferrocene as the standard.

Charge densities at open circuit and intensity modulated photovoltage spectroscopy (IMVS) were performed on a Zennium electrochemical workstation (ZAHNER, Germany), which includes a green light emitting diode (LED, 532 nm) and the corresponding control system. The intensity-modulated spectra were measured at room temperature with light intensity ranging from 5 to 75 W $m^{-2}$, in modulation frequency ranging from 0.1 Hz to 10 kHz, and with modulation amplitude less than 5% of the light intensity.

**Fabrication and Characterization of DSCs.** A double layer titania film made via screen-printing on a precleaned fluorine-doped tin oxide (FTO) conducting glass (Nippon Sheet Glass, Hyogo, Japan, sheet resistance of 14 Ω/sq) was deployed as the negative electrode of DSCs. A 3 μm-thick translucent layer of 25 nm sized titania particles was first deposited on a FTO glass and further covered with a 4 μm-thick light scattering layer of 200 nm sized titania particles (DHS-SLP1, Heptachroma, China). The film was dried in air at 120 °C for 30 min and calcined at 500 °C for 30 min under flowing oxygen before cooling to room temperature. The heated electrodes were impregnated with a 0.05 M titanium tetrachloride solution in a water-saturated desiccator at 70 °C for 30 min and fired again. The $TiO_2$ electrode was stained by immersing it into a 0.3 mM dye solution in a mixture of DCM/EtOH (v/v, 1:1) and kept at room temperature for 24 h to complete the sensitizer uptake. Then the sensitized electrodes were rinsed with dry ethanol and dried by a dry air flow. Pt catalyst was deposited on the FTO glass by coating with a drop of $H_2PtCl_6$ solution (40 mM in ethanol) with the heat treatment at 395 °C for 15 min to give photoanode. The sensitized electrode and Pt-counter electrode were assembled into a sandwich type cell by a 25 μm-thick Surlyn (DuPont) hot-melt gasket and sealed up by heating. Electrolyte Co-phen: 0.25 M [Co(II) $(phen)_3](PF_6)_2$, 0.05 M [Co(III) $(phen)_3](PF_6)_3$, 0.5 M TBP and 0.1 M LiTFSI in acetonitrile.

The photocurrent−voltage ($J$−$V$) characteristics of the solar cells were carried out using a Keithley 2400 digital source meter controlled by a computer and a standard AM1.5 solar simulator, Oriel 91160-1000 (300 W) solar simulator 2 × 2 beam. The light intensity was calibrated by an Oriel reference solar cell. A metal mask with an aperture area of 0.19 $cm^2$ was covered on a testing cell during all measurements. The action spectra of monochromatic incident photon-to-current conversion efficiency (IPCE) for solar cell were performed by using a commercial setup (QTest Station 2000 IPCE Measurement System, CROWNTECH, USA).

## RESULTS AND DISCUSSION

**Synthesis of Sensitizers.** As depicted in Scheme 1, M43, M44, M45 and M46 were prepared according to a previously reported procedure of the Buchwald−Hartwig cross-coupling of a secondary amine (**1a**−**c** and **5**) with a bromine substituted aromatic aldehyde (**2**), and the Knoevenagel condensation. Note that the Buchwald−Hartwig amination of bromine substituted aromatic aldehyde **2** must be carried out before Buchwald−Hartwig amination of 3,3′-dibromo-2,2′-bithiophene for facile synthesis of compound **9**.

**Photophysical Properties.** The electronic absorption spectra of diluted $CH_2Cl_2$ solutions of these dyes were recorded to evaluate the photophysical properties of dyes, and the corresponding properties are summarized in Table 1. As depicted in Figure 3a, the major absorption peaks for M43, M44, M45 and M46 are at 529, 535, 521 and 510 nm, respectively. A red-shifted maximum absorption wavelength along with enhanced maximum molar absorption coefficient ($\varepsilon$) 79.6 × $10^3$ $M^{-1}$ $cm^{-1}$ at 521 nm was measured for the M45


DOI: 10.1021/acsami.5b06481
ACS Appl. Mater. Interfaces 2015, 7, 22436−22447

dye, compared to that of 69.3 × $10^3$ $M^{-1}$ $cm^{-1}$ at 510 nm for M46. Clearly, the introduction of a DTP electron donor in the dithiophenepyrrole direction leads to a broadening of the absorption in comparison to the pyrrole direction. So we think the conjugation is more delocalized in the dithiophenepyrrole direction in comparison to the pyrrole direction, which results in stronger charge transfer interactions in M45 and enhanced maximum molar absorption coefficient. In spite of the slight blue shift of maximum absorption wavelength in comparison with the M43/44, the M45 dye exhibits a stronger and broader absorption.

The absorption spectra of dyes on 3 $\mu$m-thick $TiO_2$ films are shown in Figure 3b. Compared with the absorption spectrum in DCM solution, the ICT band for these sensitizers are blue-shifted (39, 41, 59 and 23 nm for M43, M44, M45 and M46, respectively), which is due to the deprotonation of the carboxylic acid.[43] In particular, the ICT band for M45 sensitized film hypsochomically shifts to 462 nm by 59 nm, which is larger than that those of M43/44. A possible reason for this observation is that M43/44 have a stronger amine donor due to the presence of mutually trans amine groups, which increases the donor strength and countervails the deprotonation effect when anchoring sensitizers onto nanocrystalline $TiO_2$ surface. Nevertheless, the hypsochomically shift of M46 sensitized film is only 23 nm, indicative of the DTP conjugation in the dithiophenepyrrole direction is more efficient than that of the pyrrole direction. Note that M45 has a higher absorbing intensity when compared to that of other dyes, which would facilitate the light harvesting of DSCs. Although M43 displays a lower absorbing intensity, primarily owing to relatively low dye load amounts. The measured dye load amounts of M43, M44, M45 and M46 are estimated to be 2.7 × $10^{-8}$, 3.4 × $10^{-8}$, 3.7 × $10^{-8}$ and 3.9 × $10^{-8}$ mol $cm^{-2}$, respectively.

We further recorded the wavelength dependent light-harvesting efficiencies of dye-grafted titania films (Figure 4),

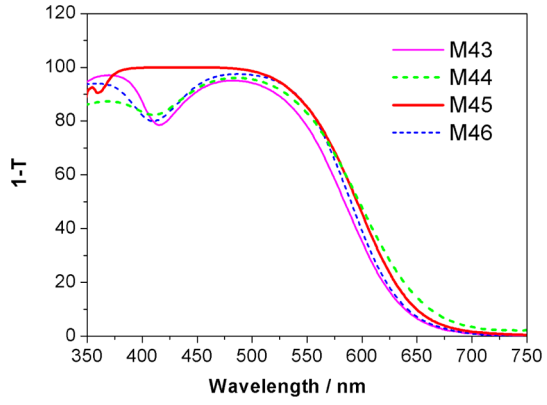


**Figure 4.** Light-harvesting efficiencies plotted vs wavelength ($\lambda$) for the 3 $\mu$m thick, dye-grafted mesoporous titania films immersed in a Co-phen electrolyte.

which was also immersed in a tris(1,10-phenanthroline) cobalt (Co-phen) electrolyte. For its detailed composition, see the Experimental Section. For the herein studied DTP electron donor, it is noted that the introduction of a DTP electron donor in the dithiophenepyrrole direction (M45) is effective in promoting a broad absorption spectral response fill the valley between 375 and 500 nm. By contrast, other dyes sensitized films lack absorptions in this region. Moreover, M45 sensitized film displays a comparable absorption at 550−700 nm with respect to those of other dyes. It is therefore a convenient sensitizer for cobalt cells using relatively thin (2−5 $\mu$m) $TiO_2$ films. The observed onset of absorption of M44 sensitized films was slightly red-shifted as compared with those for other dyes, in agreement with the results of solution absorption measurements.

To determine if there was any difference in electron donor conjugation for M45 and M46, we carried out quantum calculation with the density functional theory (DFT). Optimized ground-state molecular geometries of M45 and M46 were shown in Figure 5a. M46 possesses a large dihedral

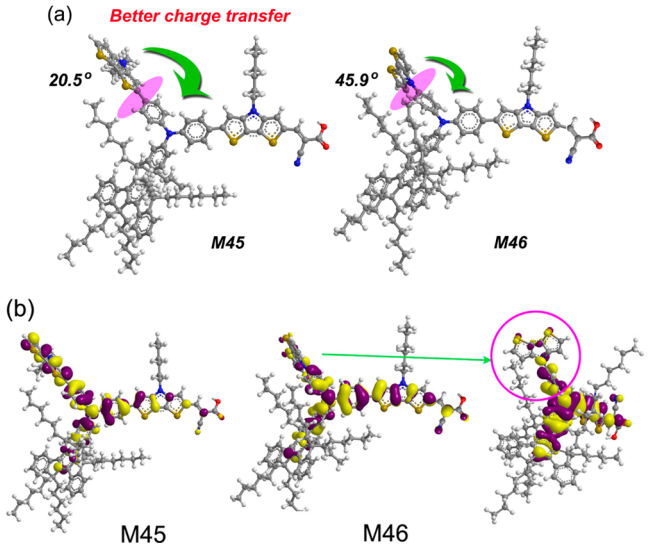


**Figure 5.** Optimized ground-state molecular geometries (a) and HOMO orbitals (b) of M45 and M46.

angle of 45.9° between the phenyl and DTP units due to the steric hindrance, whereas the corresponding dihedral angle in M45 was only 20.5° along with the conjugation alternation from the pyrrole direction to the dithiophenepyrrole direction. Therefore, the conjugation of the DTP donor with arylamine is more delocalized in the dithiophenepyrrole direction in comparison to the pyrrole direction, which results in stronger charge transfer interactions in M45 and bathochromically shifted the absorption band.

To gain insight into the charge transfer in both dyes, DFT calculations and time-dependent DFT (TDDFT) calculations of the excited states were performed. We optimized the molecular structure of M43−46 in the vacuo, and the isodensity surface plots of HOMO and LUMO are presented in Figure S2. For all these four dyes stem completely or mainly from the charge transfer transition from HOMO to LUMO. For M45, the HOMO is delocalized throughout the entire molecule, with maximum components on the triarylamine unit and the DTP donor; however the contribution from the DTP donor in M46 is much less than that of M45 (Figure 5b), which further confirm the charge transfer interactions difference in M45 and M46.

**Electrochemical Properties.** Electrochemical properties of the four dye-sensitized $TiO_2$ films were investigated by cyclic voltammetry (CV) in acetonitrile solution containing 0.1 M tetrabutylammonium perchlorate (TBAP, 0.1 M) as the supporting electrolyte (Figure 6a−c). The derived energy levels are tabulated in Table 1. The potential was externally calibrated by ferrocenium/ferrocene ($Fc^+$/Fc) couple, and then


DOI: 10.1021/acsami.5b06481
ACS Appl. Mater. Interfaces 2015, 7, 22436−22447

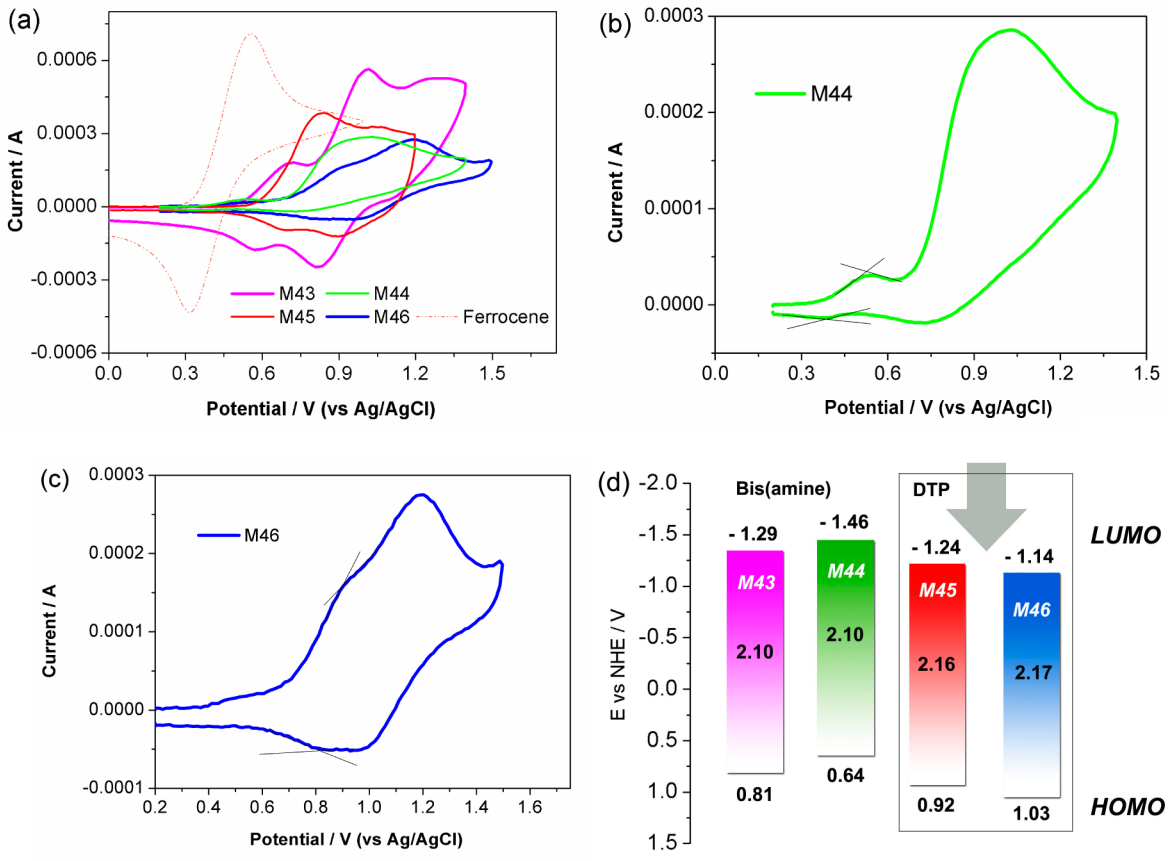


**Figure 6.** (a) CV of dyes sensitized films in MeCN with 0.1 M TBAP as the supporting electrolyte (CVs of those dyes in solutions can be found in Figure S3). (b) CV of M44 sensitized film. (c) CV of M46 sensitized film. (d) HOMO, LUMO and energy gap of studied dyes based on CV measurements.

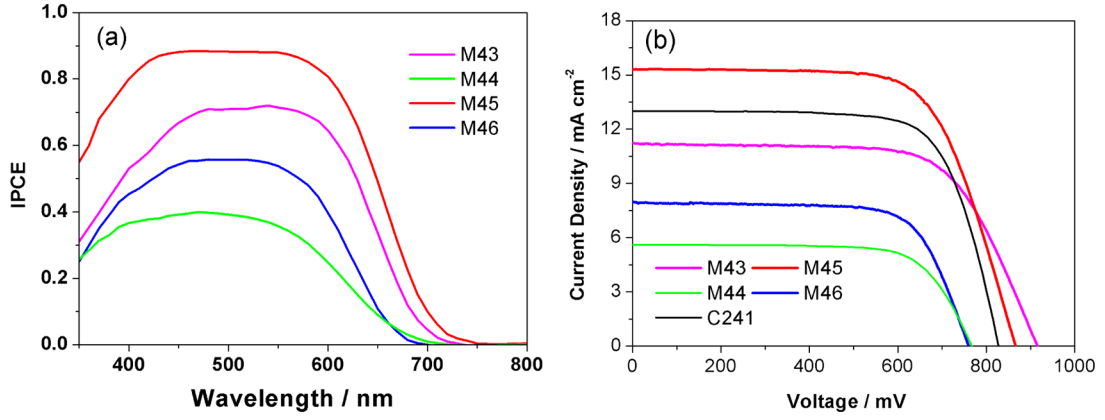


**Figure 7.** IPCE action spectra (a) and the *J*–*V* curves (b) of the studied devices employing the Co-phen electrolyte.

was calculated vs the normal hydrogen electrode (NHE) electrode ($E_{1/2}$ ($Fc^+$/Fc) = 0.63 V vs NHE). The first oxidation potential, which corresponds to the highest occupied molecular orbital (HOMO) level of M43, M44, M45 and M46 sensitized films are determined to be 0.81, 0.64, 0.92 and 1.03 V (vs NHE), respectively. With the aid of density functional theory (DFT) calculation, we obtained the calculated HOMO values of the four dyes, which increases in the order of M46 < M45 < M43 < M44 (see Table 1). A sequence that is consistent with the result of CV measurements.

Apparently, as shown in Figure 6b, the DPT donor has a more profound influence on the HOMO downward movement than those of attaching the bis(amine) moieties. Furthermore, it is noted that the DTP electron donor bringing for a broader LUMO/HOMO energy gap of 2.16 and 2.17 eV for M45 and M46, respectively. Recent studies have shown that the photocurrent of DSCs based on CoII/III polypyridyl electrolytes is dependent on the driving force for regeneration ($\Delta G_{reg}$).[69] Therefore, in view of the HOMO level, introduction of bis(amine) such as DFBA or DHBA unit has a negative effect on dye regeneration and the photocurrent of the cobalt cells. Furthermore, it can be found that both the first and the second oxidative potential values of M46 are higher than those for M45. Because higher electron density of electron donor


DOI: 10.1021/acsami.5b06481
ACS Appl. Mater. Interfaces 2015, 7, 22436−22447

results in a lower oxidative potential, this result suggested a stronger charge transfer interactions of M45 as compared to that of the M46, which is consistent with the preceding absorption spectra data and computational analysis.

**Photovoltaic Performance.** We further carried out the incident photon-to-collected electron conversion efficiency (IPCE) measurement of a dye-coated titania film in conjunction with a Co-phen electrolyte. As depicted in Figure 7a, the M46 sensitized device exhibits lower than 56% IPCEs in the wavelength range from 350 to 700 nm, whereas the noticeably enhanced IPCEs of the M45 cell in the whole visible region clearly embody the merit of introduction of DTP electron donor in the dithiophenepyrrole direction. The maximum IPCE value for DSC based on the sensitizer M43 is much lower than that for M45, which should be mainly attributed to the low dye load amounts as a result of bulky structure of DFBA. Moreover, a more negative HOMO level (0.11 V vs NHE relative to M45) may induce an insufficient driving force for the dye regeneration. Consequently, M43 sensitized DSCs tends to have a lower IPCE as compared to that of M45. Finally, the relatively low IPCE values observed for the M44 sensitized cells were likely related to the strong charge recombination between the injected electron and the oxidized dyes and/or cobalt(III) ions in electrolyte (see electron lifetime measurements). It should be noted that the HOMO level of dyes may have a significant influence on the charge recombination in DSCs. M44 has the highest HOMO level among all, which disfavors the dye regeneration and may result in recombination of the injected electrons with the oxidized dyes. In good agreement with the absorption spectra (Figure 3 and Figure 4), M45 presented higher IPCEs than those of M43 and M44 below 450 nm.

The current−voltage ($J$−$V$) characteristics of these devices under simulated one-sun illumination (AM 1.5 G, 100 mW cm$^{-2}$) are presented in Figure 7b, and the corresponding photovoltaic data are summarized in Table 2. The short-circuit photocurrent density ($J_{SC}$), open circuit photovoltage ($V_{OC}$) and fill factor (FF) of the M46 cell are 7.97 mA cm$^{-2}$, 760 mV and 0.71, respectively, affording a power conversion efficiency (PCE) of 4.30%. By contrast, a notably improved $J_{SXC}$ of 15.3 mA cm$^{-2}$ concomitant with an increased $V_{OC}$ of 867 mV was achieved with the M45 dye, contributing to a very promising efficiency as high as 9.02%. The key observation here is that a subtle modification of the electron donor direction of DTP unit induces strikingly large $J_{SC}$ and $V_{OXC}$ improvements. Under the same conditions, M43 and M44 yield PCEs of 6.97% and 2.95%, respectively. Evidently, electron donor of these dyes significantly influenced the photovoltaic properties of the dyes.

**Table 2. Photovoltaic parameters for DSCs employing the Co-phen electrolyte.**[a]

| dye | $J_{SC}$ (mA cm$^{-2}$) | $V_{OC}$ (mV) | FF | PCE (%) |
|---|---|---|---|---|
| M43 | 11.2 ± 0.3 | 915 ± 8 | 0.68 ± 0.01 | 6.97 ± 0.3 |
| M44 | 5.6 ± 0.3 | 765 ± 5 | 0.69 ± 0.01 | 2.95 ± 0.3 |
| M45 | 15.3 ± 0.3 | 867 ± 10 | 0.68 ± 0.01 | 9.02 ± 0.2 |
| M46 | 7.97 ± 0.4 | 760 ± 9 | 0.71 ± 0.01 | 4.30 ± 0.3 |
| C241 | 13.0 ± 0.4 | 830 ± 10 | 0.69 ± 0.01 | 7.44 ± 0.2 |

[a]Irradiating light: AM 1.5G (100 mW cm$^{-2}$). The photovoltaic parameters are averaged values obtained from analysis of the $J$−$V$ curves of three identical working electrodes for each device fabricated and characterized under the same experimental conditions.

Note that, M45 affords much higher photocurrent as compared that of M43/44, indicating that DTP is a powerful electron donor can successfully obtain a high photocurrent for the cobalt cells. To enable comparison with prior work by other groups, we recorded the $J$−$V$ curves of C241 (the structure can be found in Figure S4 in the Supporting Information) sensitized DSCs. The dye reported by Wang and co-workers[70] gave a PCE of 7.44% under the same conditions (Table 2).

Because the stability is extremely important for the dyes, the stability tests of the studied dyes were carried out for a few days. Figure S5 shows the variations of photovoltaic parameters ($J_{SC}$, $V_{OC}$, FF and PCE) with aging time for the DSCs employing the liquid Co-phen electrolyte. Under visible-light soaking, the PCEs of M43, M44, M45 and M46 sensitized cells decreased by 29.8%, 51.8%, 16.2% and 32.4%, respectively, after 120 h. Apparently, the photostability of M45 is better than other dyes. By contrast, M44 is less stable; and its poor efficiency may suffer from this.

To understand the discrepancy in photocurrent of these dyes, nanosecond-to-millisecond transient absorption measurements (Figure 8) were further executed. The wavelengths of pump pulses are 540 nm for the M45 samples. The pump wavelengths are selected in terms of a 0.5 optical density of the testing sample, and the pulse fluence is kept at 21.8 $\mu$J cm$^{-2}$ to afford an alike distribution profile of excitons. The solid lines are fittings of normalized absorption ($\Delta A$) via the stretched exponential decay function of $\Delta A \propto A_0 \exp[-(t/\tau)^{\alpha}]$, where $A_0$ is the pre-exponential factor, $\alpha$ is the stretching parameter and $\tau$ is the characteristic time. By use of the gamma function $\Gamma(x)$, the averaged-times of these charge transfer reactions were derived through $\tau_a = (\tau/\alpha)\Gamma(1/\alpha)$. The transient absorption of the oxidized dyes indicates the decay rates of oxidized dye caused either by regeneration or electron recombination. From the transient absorption traces of DSCs employing the Co-phen and inert electrolyte, the average time constants can be derived through stretched exponential fitting. The regeneration efficiency ($\eta_{reg}$) was estimated by using the determined averaged-times ($\tau_a$, i.e., $\tau_{redox}$ and $\tau_{inert}$) with eq 1:[69]

$$\eta_{reg} = 1 - \frac{\tau_{redox}}{\tau_{inert}} \quad (1)$$

The regeneration efficiency of the M43, M45 and M46 sensitized DSCs are calculated to be 80%, 95% and 59%, respectively. Clearly, high regeneration efficiency of M43 and M45 contributed to their good photocurrents. In addition, the low regeneration efficiency of M46 should be responsible for the moderate $J_{SC}$ values because of enhanced recombination reaction. Unfortunately, we could not obtain the regeneration efficiency of the M44, because the $\tau_{redox}$ of M44 is larger than $\tau_{inert}$. As a matter of fact, sometimes this problem can be found for other organic dyes during measurements, and the reasons are not clear.

In spite of that, we suspect that the regeneration efficiency of M44 should be lower than other dyes. The validity of this deduction could be further examined by investigating the effect of driving force for regeneration on the photocurrent performance of these dyes. $[Co(bpy)_3]^{2+/3+}$ (0.56 V vs NHE) and $[Co(dmbpy)_3]^{2+/3+}$ (0.43 V vs NHE) with higher with more negative redox potentials were employed as the electrolyte, and the detailed parameters are presented in Table S1. As expected, the $J_{SC}$ value increased with increasing of driving force for regeneration. However, M43−46 sensitized devices increased in different degrees. As Figure S6 presents, for


DOI: 10.1021/acsami.5b06481
ACS Appl. Mater. Interfaces 2015, 7, 22436−22447

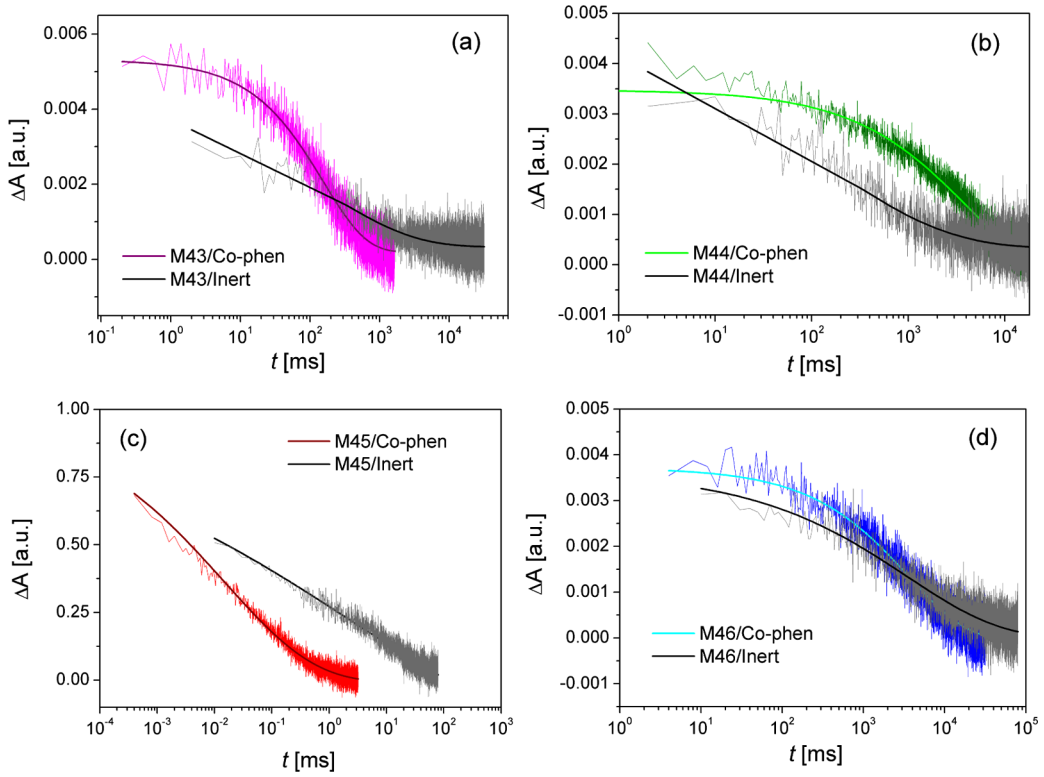


**Figure 8.** Absorption decays at a probe wavelength of 785 nm upon 5 ns laser excitation for the 4.2 $\mu$m-thick, mesoporous titania films grafted with M43 (a), M44 (b), M45 (c) and M46 (d), which are also immersed in the inert electrolyte and the Co-phen electrolyte.

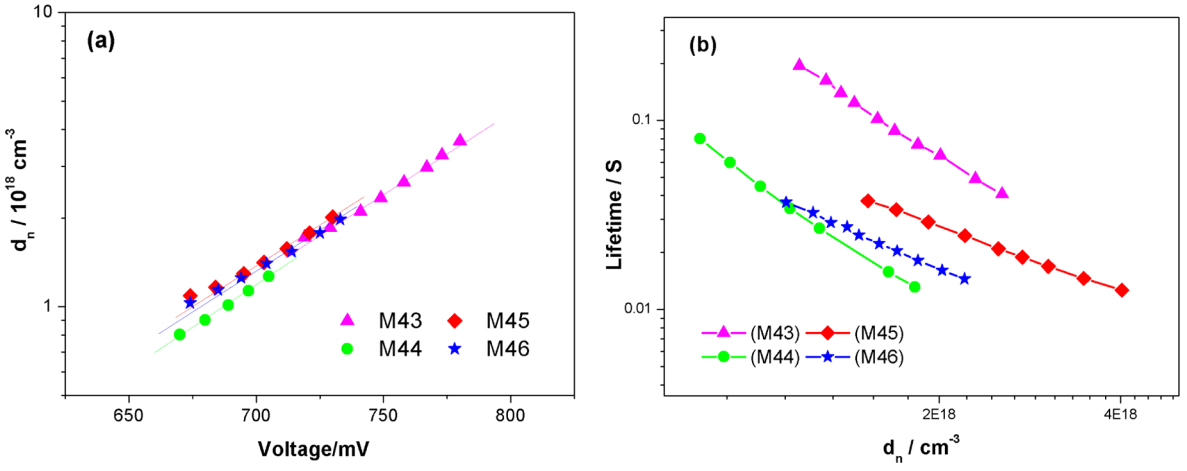


**Figure 9.** (a) Charge density at open circuit and (b) electron lifetime as a function of charge density for DSCs.

the M44-based devices, electrolyte alteration from Co-phen to Co-bpy/Co-dmbpy has caused a remarkably enhanced charge photogeneration; whereas M43 and M45 confers a moderate increase in photocurrent. This result indicates that the $J_{SC}$ performance of M44 is strongly dependent on the driving force for regeneration. In other words, the regeneration efficiency of M44 is low in the Co-phen system.

Apparently, the electron donor also has a distinct impact on the photovoltage of the devices. Surprisingly, the superior performance of BZ-HDTP as a donor relative to BZDTP in terms of the $V_{OC}$ is particularly noteworthy. It is well documented that for DSCs with an invariable redox electrolyte their $V_{OC}$ values under light are intimately related to the electron quasi-Fermi levels ($E_{F,n}$) of titania, which are determined by the density of photoinjected electrons in titania and/or the conduction band edge ($E_{CB}$) of titania.[15] To examine the dynamic origins of the change in $V_{OC}$, we performed charge-extraction and transient photovoltage decay measurements. As illustrated in Figure 9a, at fixed extracted charge density ($d_n$), the $V_{OC}$ values of M43−46 sensitized devices are very close, which indicates that the conduction-band edge ($E_c$) of these dye-sensitized films are nearly unchanged.

Figure 9b shows the electron lifetime ($\tau$) as a function of extracted charge density at open circuit for the cobalt cells. For M46, a shorter electron lifetime has been measured compared to devices incorporating M45, giving a clear clue regarding its smaller photovoltage and photocurrent. At a fixed Q ($1.92 \times 10^{18}$ cm$^3$), the $\tau$ value for M45-based DSCs is larger than that of M46-based DSCs by around 1.6-fold. This indicates that charge recombination between injection electrons the oxidized


DOI: 10.1021/acsami.5b06481
ACS Appl. Mater. Interfaces 2015, 7, 22436−22447

dyes and/or cobalt(III) ions in electrolyte in the M46 cells is stronger than those of the M45 cells. The significantly attenuated rates of charge-recombination gave birth to an 107 mV increase in $V_{OC}$ at an irradiance of 100 mW cm$^{-2}$ simulated AM 1.5 sunlight from 760 mV for M46 to 867 mV for M45. Meanwhile, the controlled charge recombination contributes to $J_{SC}$ because of the improved charge collection efficiency at the photoanode, leading to a photocurrent increase of 91.9% as compared to the M46. Furthermore, the dye alteration from M45 to M43 has caused a 2.4-fold increased electron lifetime. Therefore, it is concluded that the observed enhancement of $V_{OC}$ from M45 to M43 dye is attributed to the effect of retarded charge recombination.

The superiority of M45 with respective to M46 regarding reduction of charge recombination can be understood from the structure of the molecule. The most apparent structure difference of M45 from M46 is the DTP donor of the molecule. As illustrated in Figure 10, the DTP "arm" in the

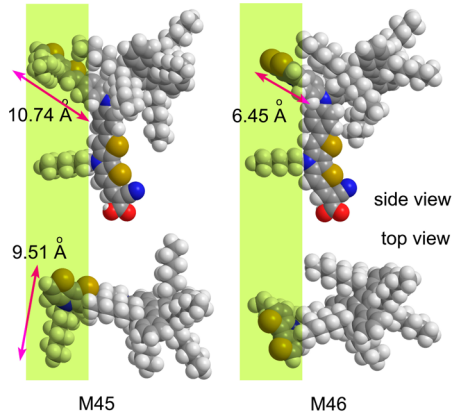


**Figure 10.** Molecular structures of M45 and M46 derived from density functional theory (DFT) calculations (b3lyp).

yellow region for M45 (10.74 Å) is longer than that of the M46 (6.45 Å), regarding the side view of the molecule. Importantly, M45 possess a long alkyl chain in its DTP donor, whereas M46 lacks the alkyl chain in this part. Note that the significant effect of alkyl chains on controlling the rate of recombining photoinjected electrons with holes of the electrolyte and/or the oxidized state of dye molecules is widely recognized.[2,3,43,50] Thus, the bulkier structure of M45 increases the steric hindrance, which blocks the approach of the oxidized dyes and/or cobalt(III) ions in electrolyte to $TiO_2$ film.

## CONCLUSIONS

In summary, we incorporated dithieno[3,2-b:2′,3′-d]pyrrole and two bis(amine) units as the terminal donor to develop novel D−D−$\pi$−A organic sensitizers. The introduction of DTP in the dithiophenepyrrole direction has several advantages, such as increasing the maximum molar absorption coefficient and extending the absorption bands, enhancing charge transfer interaction and beneficial to photocurrent generation. In conjunction with the Co-phen electrolyte, M45 yielded PCEs of 9.02% at the 100 mW cm$^{-2}$, simulated AM1.5 conditions. The outstanding IPCE response and high energy conversion efficiency of M45 sensitized cobalt cells indicates that the N,S-heterocycles such as DTP unit could be a promising candidate for application in highly efficient D−D−$\pi$−A organic sensitizers. Also, these results trigger new ideas for designing more promising highly efficient dyes toward the cobalt electrolytes.

## ASSOCIATED CONTENT

### Supporting Information

The Supporting Information is available free of charge on the ACS Publications website at DOI: 10.1021/acsami.5b06481.

$^1$H NMR spectra of new compounds (Figures S7−15) (PDF).

## AUTHOR INFORMATION

### Corresponding Authors

*M. Liang. E-mail: liangmao717@126.com.
*P. Wang. E-mail: peng.wang@ciac.jl.cn.

### Author Contributions

The paper was written through contributions of all authors. All authors have given approval to the final version of the paper.

### Notes

The authors declare no competing financial interest.

## ACKNOWLEDGMENTS

We gratefully acknowledge the financial support from the National Science Foundation of China (No. 21373007, 21376179), and the Tianjin Natural Science Foundation (13JCZDJC32400, 14JCYBJC21400).

## REFERENCES

(1) O'Regan, B.; Grätzel, M. High-Efficiency Solar Cell Based on Dye-Sensitized Colloidal $TiO_2$ Films. *Nature* **1991**, *353*, 737−740.
(2) Hagfeldt, A.; Boschloo, G.; Sun, L.; Kloo, L.; Pettersson, H. Dye Sensitized Solar Cells. *Chem. Rev.* **2010**, *110*, 6595−6663.
(3) Liang, M.; Chen, J. Arylamine Organic Dyes for Dye-Sensitized Solar Cells. *Chem. Soc. Rev.* **2013**, *42*, 3453−3488.
(4) Lee, C.-P.; Lin, R. Y.-Y.; Lin, L.-Y.; Li, C.-T.; Chu, T.-C.; Sun, S.-S.; Lin, J. T.; Ho, K.-C. Recent Progress in Organic Sensitizers for Dye-Sensitized Solar Cells. *RSC Adv.* **2015**, *5*, 23810−23825.
(5) Omata, K.; Kuwahara, S.; Katayama, K.; Qing, S.; Toyoda, T.; Lee, K.−M.; Wu, C.−G. The Cause for the Low Efficiency of Dye Sensitized Solar Cells with a Combination of Ruthenium Dyes and Cobalt Redox. *Phys. Chem. Chem. Phys.* **2015**, *17*, 10170−10175.
(6) Lu, X. F.; Lan, T.; Qin, Z. W.; Wang, Z.-S.; Zhou, G. A Near-Infrared Dithieno[2,3-a:3′,2′-c]phenazine-Based Organic Co-Sensitizer for Highly Efficient and Stable Quasi-Solid-State Dye-Sensitized Solar Cells. *ACS Appl. Mater. Interfaces* **2014**, *6*, 19308−19317.
(7) Wang, Y.; Chen, B.; Wu, W.; Li, X.; Zhu, W.; Tian, H.; Xie, Y. Efficient Solar Cells Sensitized by Porphyrins with an Extended Conjugation Framework and a Carbazole Donor: From Molecular Design to Cosensitization. *Angew. Chem., Int. Ed.* **2014**, *53*, 10779−10783.
(8) Lin, R. Y.-Y.; Lin, H.-W.; Yen, Y.-S.; Chang, C.-H.; Chou, H.-H.; Chen, P.-W.; Hsu, C.-Y.; Chen, Y.-C.; Lin, J.-T.; Ho, K.-C. 2,6-Conjugated Anthracene Sensitizers for High-Performance Dye-Sensitized Solar Cells. *Energy Environ. Sci.* **2013**, *6*, 2477−2486.
(9) Yang, L.; Zheng, Z.; Li, Y.; Wu, W. J.; Tian, H.; Wang, Z. H. N-Annulated Perylene-based Metal-Free Organic Sensitizers for Dye-Sensitized Solar Cells. *Chem. Commun.* **2015**, *51*, 4842−4845.
(10) Xu, M.; Zhou, D.; Cai, N.; Liu, J.; Li, R.; Wang, P. Electrical and Photophysical Analyses on the Impacts of Arylamine Electron Donors in Cyclopentadithiophene Dye-Sensitized Solar Cells. *Energy Environ. Sci.* **2011**, *4*, 4735−4742.
(11) Baheti, A.; Thomas, K. R. J.; Li, C.-T.; Lee, C.-P.; Ho, K.-C. Fluorene-Based Sensitizers with a Phenothiazine Donor: Effect of Mode of Donor Tethering on the Performance of Dye-Sensitized Solar Cells. *ACS Appl. Mater. Interfaces* **2015**, *7*, 2249−2262.


DOI: 10.1021/acsami.5b06481
*ACS Appl. Mater. Interfaces* 2015, 7, 22436−22447

(12) Cong, J. Y.; Hao, Y.; Boschloo, G.; Kloo, L. Electrolytes Based on TEMPO-Co Tandem Redox Systems Outperform Single Redox Systems in Dye-sensitized Solar Cells. *ChemSusChem* **2015**, *8*, 264−268.
(13) Huang, Z.-S.; Feng, H.-L.; Zang, X.-F.; Iqbal, Z.; Zeng, H.; Kuang, D.-B.; Wang, L.; Meier, H.; Cao, D. Dithienopyrrolobenzothiadiazole-based Organic Dyes for Efficient Dye-Sensitized Solar Cells. *J. Mater. Chem. A* **2014**, *2*, 15365−15376.
(14) Liang, Y.; Cheng, F.; Liang, J.; Chen, J. Triphenylamine-Based Ionic Dyes with Simple Structures: Broad Photoresponse and Limitations on Open-Circuit Voltage in Dye-Sensitized Solar Cells. *J. Phys. Chem. C* **2010**, *114*, 15842−15848.
(15) Marinado, T.; Nonomura, K.; Nissfolk, J.; Karlsson, M. K.; Hagberg, D. P.; Sun, L.; Mori, S.; Hagfeldt, A. How the Nature of Triphenylamine-Polyene Dyes in Dye-Sensitized Solar Cells Affects the Open-Circuit Voltage and Electron Lifetimes. *Langmuir* **2010**, *26*, 2592−2598.
(16) Qian, X.; Zhu, Y.-Z.; Chang, W.-Y.; Song, J.; Pan, B.; Lu, L.; Gao, H.-H.; Zheng, J.-Y. Benzo[a]carbazole-Based Donor−π−Acceptor Type Organic Dyes for Highly Efficient Dye-Sensitized Solar Cells. *ACS Appl. Mater. Interfaces* **2015**, *7*, 9015−9022.
(17) Gao, P.; Tsao, H. N.; Yi, C. Y.; Grätzel, M.; Nazeeruddin, M. K. Extended π-Bridge in Organic Dye-Sensitized Solar Cells: the Longer, the Better? *Adv. Energy Mater.* **2015**, *4*, DOI: 10.1002/aenm.201301485.
(18) Gao, P.; Kim, Y. J.; Yum, J.-H.; Holcombe, T. W.; Nazeeruddin, M. K.; Grätzel, M. Facile Synthesis of A Bulky BPTPA Donor Group Suitable for Cobalt Electrolyte based Dye Sensitized Solar Cells. *J. Mater. Chem. A* **2013**, *1*, 5535−5544.
(19) Hua, Y.; Chang, S.; Huang, D. D.; Zhou, X.; Zhu, X. J.; Zhao, J. Z.; Chen, T.; Wong, W. Y.; Wong, W. K. Significant Improvement of Dye-Sensitized Solar Cell Performance Using Simple Phenothiazine-Based Dyes. *Chem. Mater.* **2013**, *25*, 2146−2153.
(20) Zhou, N. J.; Prabakaran, K.; Lee, B.; Chang, S. H.; Harutyunyan, B.; Guo, P. J.; Butler, M. R.; Timalsina, A.; Bedzyk, M. J.; Ratner, M. A.; Vegiraju, S.; Yau, S.; Wu, C.-G.; Chang, R. P. H.; Facchetti, A.; Chen, M.-C.; Marks, T. J. Metal-Free Tetrathienoacene Sensitizers for High-Performance Dye-Sensitized Solar Cells. *J. Am. Chem. Soc.* **2015**, *137*, 4414−4423.
(21) Yella, A.; Humphry-Baker, R.; Curchod, B. F. E.; Astani, N. A.; Teuscher, J.; Polander, L. E.; Mathew, S.; Moser, J.-E.; Tavernelli, I.; Rothlisberger, U.; Grätzel, M.; Nazeeruddin, M. K.; Frey, J. Molecular Engineering of a Fluorene Donor for Dye-Sensitized Solar Cells. *Chem. Mater.* **2013**, *25*, 2733−2739.
(22) Nguyen, W. H.; Bailie, C. D.; Burschka, J.; Moehl, T.; Grätzel, M.; McGehee, M. D.; Sellinger, A. Molecular Engineering of Organic Dyes for Improved Recombination Lifetime in Solid-State Dye-Sensitized Solar Cells. *Chem. Mater.* **2013**, *25*, 1519−1525.
(23) Kang, X.; Zhang, J.; O'Neil, D.; Rojas, A. J.; Chen, W.; Szymanski, P.; Marder, S. R.; El-Sayed, M. A. Effect of Molecular Structure Perturbations on the Performance of the D-A-π-A Dye Sensitized Solar Cells. *Chem. Mater.* **2014**, *26*, 4486−4493.
(24) Qi, Q. B.; Wang, X. Z.; Fan, L.; Zheng, B.; Zeng, W. D.; Luo, J.; Huang, K.-W.; Wang, Q.; Wu, J. S. N-Annulated Perylene-Based Push-Pull-Type Sensitizers. *Org. Lett.* **2015**, *17*, 724−727.
(25) Tan, Y. L.; Liang, M.; Lu, Z. Y.; Zheng, Y. Q.; Tong, X. L.; Sun, Z.; Xue, S. Novel Triphenylamine Donors with Carbazole Moieties for Organic Sensitizers toward Cobalt(II/III) Redox Mediators. *Org. Lett.* **2014**, *16*, 3978−3981.
(26) Chou, C. C.; Hu, F. C.; Yeh, H. H.; Wu, H. P.; Chi, Y.; Clifford, J. N.; Palomares, E.; Liu, S. H.; Chou, P. T.; Lee, G. H. Highly Efficient Dye-Sensitized Solar Cells Based on Panchromatic Ruthenium Sensitizers with Quinolinylbipyridine Anchors. *Angew. Chem., Int. Ed.* **2014**, *53*, 178−183.
(27) Sun, Z.; Zhang, R.-K.; Xie, H.-H.; Wang, H.; Liang, M.; Xue, S. Nonideal Charge Recombination and Conduction Band Edge Shifts in Dye-Sensitized Solar Cells Based on Adsorbent Doped Poly(ethylene oxide) Electrolytes. *J. Phys. Chem. C* **2013**, *117*, 4364−4373.
(28) Lu, J.; Chang, Y.-C.; Cheng, H.-Y.; Wu, H.-P.; Cheng, Y.; Wang, M.; Diau, E. W.-G. Molecular Engineering of Organic Dyes with a Hole-Extending Donor Tail for Efficient All-Solid-State Dye-Sensitized Solar Cells. *ChemSusChem* **2015**, *8*, 2529−2536.
(29) Yella, A.; Lee, H.; Tsao, H.; Yi, C.; Chandiran, A.; Nazeeruddin, M.; Diau, E.; Yeh, C.; Zakeeruddin, S.; Grätzel, M. Porphyrin-Sensitized Solar Cells with Cobalt (II/III)-Based Redox Electrolyte Exceed 12% Efficiency. *Science* **2011**, *334*, 629−634.
(30) Kashif, M. K.; Nippe, M.; Duffy, N. W.; Forsyth, C. M.; Chang, C. J.; Long, J. R.; Spiccia, L.; Bach, U. Stable Dye-Sensitized Solar Cell Electrolytes Based on Cobalt(II)/(III) Complexes of A Hexadentate Pyridyl Ligand. *Angew. Chem.* **2013**, *125*, 5637−5641.
(31) Feldt, S. M.; Gibson, E. A.; Gabrielsson, E.; Sun, L.; Boschloo, G.; Hagfeldt, A. Design of Organic Dyes and Cobalt Polypyridine Redox Mediators for High-Efficiency Dye-Sensitized Solar Cells. *J. Am. Chem. Soc.* **2010**, *132*, 16714−16724.
(32) Sun, Z.; Liang, M.; Chen, J. Kinetics of Iodine-Free Redox Shuttles in Dye-Sensitized Solar Cells: Interfacial Recombination and Dye Regeneration. *Acc. Chem. Res.* **2015**, *48*, 1541−1550.
(33) Mathew, S.; Yella, A.; Gao, P.; Humphry-Baker, R.; Curchod, B. F. E.; Ashari-Astani, N.; Tavernelli, I.; Rothlisberger, U.; Nazeeruddin, M. K.; Grätzel, M. Dye-Sensitized Solar Cells with 13% Efficiency Achieved through the Molecular Engineering of Porphyrin Sensitizers. *Nat. Chem.* **2014**, *6*, 242−247.
(34) Kakiage, K.; Aoyama, Y.; Yano, T.; Otsuka, T.; Kyomen, T.; Unno, M.; Hanaya, M. An Achievement of over 12% Efficiency in an Organic Dye-Sensitized Solar Cells. *Chem. Commun.* **2014**, *50*, 6379−6381.
(35) Yao, Z. Y.; Zhang, M.; Wu, H.; Yang, L.; Li, R. Z.; Wang, P. Donor/Acceptor Indenoperylene Dye for Highly Efficient Organic Dye-Sensitized Solar Cells. *J. Am. Chem. Soc.* **2015**, *137*, 3799−3802.
(36) Zhang, M.; Wang, Y.; Xu, M.; Ma, W.; Li, R.; Wang, P. Design of High-Efficiency Organic Dyes for Titania Solar Cells Based on the Chromophoric Core of Cyclopentadithiophene- Benzothiadiazole. *Energy Environ. Sci.* **2013**, *6*, 2944−2949.
(37) Yao, Z.; Zhang, M.; Li, R.; Yang, L.; Qiao, Y.; Wang, P. A Metal-Free N-Annulated Thienocyclopentaperylene Dye: Power Conversion Efficiency of 12% for Dye-Sensitized Solar Cells. *Angew. Chem., Int. Ed.* **2015**, *54*, 5994−5998.
(38) Ning, Z.; Zhang, Q.; Wu, W.; Pei, H.; Liu, B.; Tian, H. Starburst Triarylamine Based Dyes for Efficient Dye-Sensitized Solar Cells. *J. Org. Chem.* **2008**, *73*, 3791−3797.
(39) Wu, Y.; Zhu, W. Organic Sensitizers from D-π-A to D-A-π-A: Effect of the Internal Electron-withdrawing Units on Molecular Absorption, Energy Levels and Photovoltaic Performances. *Chem. Soc. Rev.* **2013**, *42*, 2039−2058.
(40) Velusamy, M.; Thomas, J. K. R.; Lin, J. T.; Hsu, Y.-C.; Ho, K.-C. Organic Dyes Incorporating Low-band-gap Chromophores for Dye-sensitized Solar Cells. *Org. Lett.* **2005**, *7*, 1899−1902.
(41) Zhu, W. H.; Wu, Y.; Wang, S.; Li, W.; Li, X.; Chen, J.; Wang, Z. S.; Tian, H. Organic D-A-π-A Solar Cell Sensitizers with Improved Stability and Spectral Response. *Adv. Funct. Mater.* **2011**, *21*, 756−763.
(42) Joly, D.; Pellejà, L.; Narbey, S.; Oswald, F.; Meyer, T.; Kervella, Y.; Maldivi, P.; Clifford, J. N.; Palomares, E.; Demadrille, R. Metal-Free Organic Sensitizers with Narrow Absorption in the Visible for Solar Cells Exceeding 10% Efficiency. *Energy Environ. Sci.* **2015**, *8*, 2010−2018.
(43) Cui, Y.; Wu, Y.; Lu, X.; Zhang, X.; Zhou, G.; Miapeh, F. B.; Zhu, W. H.; Wang, Z. S. Incorporating Benzotriazole Moiety to Construct D-A-π-A Organic Sensitizers for Solar Cells: Significant Enhancement of Open-Circuit Photovoltage with Long Alkyl Group. *Chem. Mater.* **2011**, *23*, 4394−4401.
(44) Chaurasia, S.; Hung, W.-I.; Chou, H.-H.; Lin, J. T. Incorporating a New 2H-[1,2,3]Triazolo[4,5-c]pyridine Moiety to Construct D−A−π−A Organic Sensitizers for High Performance Solar Cells. *Org. Lett.* **2014**, *16*, 3052−3055.
(45) Mao, J.; Yang, J.; Teuscher, J.; Moehl, T.; Yi, C.; Humphry-Baker, R.; Comte, P.; Grätzel, C.; Hua, J.; Zakeeruddin, S. M.; Tian, H.; Grätzel, M. Thiadiazolo[3,4-c]pyridine Acceptor Based Blue


DOI: 10.1021/acsami.5b06481
*ACS Appl. Mater. Interfaces* 2015, 7, 22436−22447

Sensitizers for High Efficiency Dye-Sensitized Solar Cells. *J. Phys. Chem. C* **2014**, *118*, 17090−17099.
(46) Pei, K.; Wu, Y. Z.; Islam, A.; Zhang, Q.; Han, L. Y.; Tian, H.; Zhu, W. H. Constructing High-Efficiency D-A-π-A-Featured Solar Cell Sensitizers: a Promising Building Block of 2,3-Diphenylquinoxaline for Antiaggregation and Photostability. *ACS Appl. Mater. Interfaces* **2013**, *5*, 4986−4995.
(47) Lu, X.; Feng, Q.; Lan, T.; Zhou, G.; Wang, Z.-S. Molecular Engineering of Quinoxaline-Based Organic Sensitizers for Highly Efficient and Stable Dye-Sensitized Solar Cells. *Chem. Mater.* **2012**, *24*, 3179−3187.
(48) Lan, T.; Lu, X.; Zhang, L.; Chen, Y.; Zhou, G.; Wang, Z.-S. Enhanced Performance of Quasi-Solid-State Dye-Sensitized Solar Cells by Tuning the Building Blocks in D−(π)−A′−π−A featured Organic Dyes. *J. Mater. Chem. A* **2015**, *3*, 9869−9881.
(49) Li, W. Q.; Wu, Y. Z.; Zhang, Q.; Tian, H.; Zhu, W. H. D-A-π-A Featured Sensitizers Bearing Phthalimide and Benzotriazole as Auxiliary Acceptor: Effect on Absorption and Charge Recombination Dynamics in Dye-Sensitized Solar Cells. *ACS Appl. Mater. Interfaces* **2012**, *4*, 1822−1830.
(50) Qu, S.; Qin, C.; Islam, A.; Wu, Y.; Zhu, W.; Hua, J.; Tian, H.; Han, L. A Novel D-A-π-A Organic Sensitizer Containing a Diketopyrrolopyrrole Unit with a Branched Alkyl Chain for Highly Efficient and Stable Dye-Sensitized Solar Cells. *Chem. Commun.* **2012**, *48*, 6972−6974.
(51) Zhang, X.; Mao, J.; Wang, D.; Li, X.; Yang, J.; Shen, Z.; Wu, W.; Li, J.; Ågren, H.; Hua, J. Comparative Study on Pyrido[3,4-b]pyrazine-Based Sensitizers by Tuning Bulky Donors for Dye-Sensitized Solar Cells. *ACS Appl. Mater. Interfaces* **2015**, *7*, 2760−2771.
(52) Lu, X.; Zhou, G.; Wang, H.; Feng, Q.; Wang, Z.-S. Near Infrared Thieno[3,4-b]pyrazine Sensitizers for Efficient Quasi-Solid-State Dye-Sensitized Solar Cells. *Phys. Chem. Chem. Phys.* **2012**, *14*, 4802−4809.
(53) Dessì, A.; Calamante, M.; Mordini, A.; Peruzzini, M.; Sinicropi, A.; Basosi, R.; Fabrizi de Biani, F.; Taddei, M.; Colonna, D.; di Carlo, A.; Reginato, G.; Zani, L. Organic Dyes with Intense Light Absorption Especially Suitable for Application in Thin-layer Dye-Sensitized Solar Cells. *Chem. Commun.* **2014**, *50*, 13952−13955.
(54) Dessì, A.; Calamante, M.; Mordini, A.; Peruzzini, M.; Sinicropi, A.; Basosi, R.; Fabrizi de Biani, F.; Taddei, M.; Colonna, D.; di Carlo, A. D.; Reginato, G.; Zani, L. Thiazolo[5,4-d]thiazole-based Organic Sensitizers with Strong Visible Light Absorption for Transparent, Efficient and Stable Dye-Sensitized Solar Cells. *RSC Adv.* **2015**, *5*, 32657−32668.
(55) Guo, F.; He, J.; Qu, S.; Li, J.; Zhang, Q.; Wu, W.; Hua, J. Structure-property Relationship of Different Electron Donors: New Organic Sensitizers Based on Bithiazole Moiety for High Efficiency Dye-Sensitized Solar Cells. *RSC Adv.* **2013**, *3*, 15900−15908.
(56) Liu, W.-H.; Wu, I.-C.; Lai, C.-H.; Lai, C.-H.; Chou, P.-T.; Li, Y.-T.; Chen, C.-L.; Hsu, Y.-Y.; Chi, Y. Simple Organic Molecules Bearing a 3,4-Ethylenedioxythiophene Linker for Efficient Dye-Sensitized Solar Cells. *Chem. Commun.* **2008**, 5152−5154.
(57) Kang, X.; Zhang, J.; Rojas, A. J.; O'Neil, D.; Szymanski, P.; Marder, S. R.; El-Sayed, M. A. Deposition of Loosely Bound Organic D−A−π−A′ Dyes on Sensitized $TiO_2$ Film: a Possible Strategy to Suppress Charge Recombination and Enhance Power Conversion Efficiency in Dye-Sensitized Solar Cells. *J. Mater. Chem. A* **2014**, *2*, 11229−11234.
(58) Liu, B.; Wang, B.; Wang, R.; Gao, L.; Huo, S.; Liu, Q.; Li, X.; Zhu, W. Influence of Conjugated π-Linker in D−D−π−A Indoline Dyes: towards Long-Term Stable and Efficient Dye-Sensitized Solar Cells with High Photovoltage. *J. Mater. Chem. A* **2014**, *2*, 804−812.
(59) Tan, L.-L.; Huang, J.-F.; Shen, Y.; Xiao, L.-M.; Liu, J.-M.; Kuang, D.-B.; Su, C.-Y. Highly Efficient and Stable Organic Sensitizers with Duplex Starburst Triphenylamine and Carbazole Donors for Liquid and Quasi-Solid-State Dye-Sensitized Solar Cells. *J. Mater. Chem. A* **2014**, *2*, 8988−8994.
(60) Namuangruk, S.; Fukuda, R.; Ehara, M.; Meeprasert, J.; Khanasa, T.; Morada, S.; Kaewin, T.; Jungsuttiwong, S.; Sudyoadsuk, T.; Promarak, V. D−D−π−A-Type Organic Dyes for Dye-Sensitized Solar Cells with a Potential for Direct Electron Injection and a High Extinction Coefficient: Synthesis, Characterization, and Theoretical Investigation. *J. Phys. Chem. C* **2012**, *116*, 25653−25663.
(61) Thongkasee, P.; Thangthong, A.; Janthasing, N.; Sudyoadsuk, T.; Namuangruk, S.; Keawin, T.; Jungsuttiwong, S.; Promarak, V. Carbazole-Dendrimer-Based Donor−π−Acceptor Type Organic Dyes for Dye-Sensitized Solar Cells: Effect of the Size of the Carbazole Dendritic Donor. *ACS Appl. Mater. Interfaces* **2014**, *6*, 8212−8222.
(62) Venkateswararao, A.; Thomas, K. R. J.; Lee, C.-P.; Li, C.-T.; Ho, K.-C. Organic Dyes Containing Carbazole as Donor and π-Linker: Optical, Electrochemical, and Photovoltaic Properties. *ACS Appl. Mater. Interfaces* **2014**, *6*, 2528−2539.
(63) Wan, Z.; Jia, C.; Duan, Y.; Zhou, Li.; Lin, Y.; Shi, Y. Phenothiazine−Triphenylamine Based Organic Dyes Containing Various Conjugated Linkers for Efficient Dye-Sensitized Solar Cells. *J. Mater. Chem.* **2012**, *22*, 25140−25147.
(64) Chen, C.; Liao, J.-Y.; Chi, Z.; Xu, B.; Zhang, X.; Kuang, D.-B.; Zhang, Y.; Liu, S.; Xu, J. Metal-Free Organic Dyes Derived from Triphenylethylene for Dye-Sensitized Solar Cells: Tuning of The Performance by Phenothiazine and Carbazole. *J. Mater. Chem.* **2012**, *22*, 8994−9005.
(65) Yang, C.-J.; Chang, Y. J.; Watanabe, M.; Hon, Y.-S.; Chow, T. J. Phenothiazine Derivatives as Organic Sensitizers for Highly Efficient Dye-Sensitized Solar Cells. *J. Mater. Chem.* **2012**, *22*, 4040−4049.
(66) Wu, W.; Yang, J.; Hua, J.; Tang, J.; Zhang, L.; Long, Y.; Tian, H. Efficient and Stable Dye-Sensitized Solar Cells Based on Phenothiazine Sensitizers with Thiophene Units. *J. Mater. Chem.* **2010**, *20*, 1772−1779.
(67) Zhang, M.-D.; Xie, H.-X.; Ju, X.-H.; Qin, L.; Yang, Q.-X.; Zheng, H.-G.; Zhou, X.-F. D-D-π-A Organic Dyes containing 4,4′-Di(2-thienyl)-triphenylamine Moiety for Efficient Dye-Sensitized Solar Cells. *Phys. Chem. Chem. Phys.* **2013**, *15*, 634−641.
(68) Echeverry, C. A.; Cotta, R.; Castro, E.; Ortiz, A.; Echegoyen, L.; Insuasty, B. New Organic Dyes with High IPCE Values containing Two Triphenylamine Units as Co-Donors for Efficient Dye-Sensitized Solar Cells. *RSC Adv.* **2015**, *5*, 60823−60830.
(69) Feldt, S. M.; Lohse, P. W.; Kessler, F.; Nazeeruddin, M. K.; Grätzel, M.; Boschloo, G.; Hagfeldt, A. Regeneration and Recombination Kinetics in Cobalt Polypyridine based Dye-Sensitized Solar Cells, Explained using Marcus Theory. *Phys. Chem. Chem. Phys.* **2013**, *15*, 7087−7097.
(70) Xu, M.; Zhang, M.; Pastore, M.; Li, R.; De Angelis, F.; Wang, P. Joint Electrical, Photophysical and Computational Studies on D-π-A Dye Sensitized Solar Cells: the Impacts of Dithiophene Rigidification. *Chem. Sci.* **2012**, *3*, 976−983.


DOI: 10.1021/acsami.5b06481
*ACS Appl. Mater. Interfaces* 2015, 7, 22436−22447